

Lehigh University Lehigh Preserve

Fritz Laboratory Reports

Civil and Environmental Engineering

1976

Tests of fabricated tubular columns, January 1976. Presented at ASCE National Water Resources conf., April 1976 ASCE Preprint #2735 77-1

D. A. Ross

W. F. Chen

Follow this and additional works at: <http://preserve.lehigh.edu/engr-civil-environmental-fritz-lab-reports>

Recommended Citation

Ross, D. A. and Chen, W. F., "Tests of fabricated tubular columns, January 1976. Presented at ASCE National Water Resources conf., April 1976 ASCE Preprint #2735 77-1" (1976). *Fritz Laboratory Reports*. Paper 477.
<http://preserve.lehigh.edu/engr-civil-environmental-fritz-lab-reports/477>

This Technical Report is brought to you for free and open access by the Civil and Environmental Engineering at Lehigh Preserve. It has been accepted for inclusion in Fritz Laboratory Reports by an authorized administrator of Lehigh Preserve. For more information, please contact preserve@lehigh.edu.



TESTS OF FABRICATED TUBULAR COLUMNS

by

D. A. Ross
Research Assistant
Fritz Engineering Laboratory
Lehigh University
Bethlehem, Pa. 18015

W. F. Chen
Professor of Civil Engineering
Fritz Engineering Laboratory
Lehigh University
Bethlehem, Pa. 18015

This paper is prepared for presentation to the Structural Division of the 1976 ASCE San Diego Convention, April 5-8, 1976. Session No. 42 "Design Problems in Offshore Metal Structures"

FRITZ ENGINEERING
LABORATORY LIBRARY

January 1976

Lehigh/FL/393-7 (76)

TABLE OF CONTENTS

	<u>Page</u>
ABSTRACT	i
1. Introduction	1
2. Scope of Test Program	2
3. Preliminary Tests	3
4. Residual Stresses	4
5. Long Column Testing	7
5.1 General	7
5.2 Initial Imperfections	8
5.3 Experimental Technique	10
5.4 Results and Discussion	12
5.5 Comparison of Predicted and Observed Buckling Loads	15
6. Summary and Conclusions	16
7. Acknowledgments	19
8. References	19
9. List of Symbols	20
TABLES	22
FIGURES	27

LIST OF TABLES

Table

- 1 List of Specimens
- 2 Material Properties
- 3 Column Specimen Out-of-Straightnesses
- 4 Unintended Initial End Eccentricities
- 5 Failure Mechanism and Direction
- 6 Failure Behavior Data

LIST OF FIGURES

Figure

- 1 Longitudinal Residual Stress Distribution Obtained from Slicing Method
- 2 Circumferential Residual Stress Pattern
- 3 Circumferential Residual Stress Distribution
- 4 Comparison of Predicted and Measured Circumferential Residual Stresses
- 5 Typical Specimen Out-of-Straightness as Measured Prior to Testing
- 6 Column Testing
- 7 Axial Load-Lateral Deflection Curves at Midheight
- 8 Definition of Critical and Buckling Loads
- 9 Stub Column Predictions--Static Yield Stresses Assumed
- 10 Comparison of Test Results with Column Buckling Curves--Dynamic Yield Stresses Assumed
- 11 Comparison of Test Results with Column Buckling Curves--Static Yield Stresses Assumed

TESTS OF FABRICATED TUBULAR COLUMNS

By

D. A. Ross
Research Assistant
Fritz Engineering Laboratory
Lehigh University
Bethlehem, Pa. 18015

W. F. Chen
Professor of Civil Engineering
Fritz Engineering Laboratory
Lehigh University
Bethlehem, Pa. 18015

ABSTRACT

This paper describes an experimental program directed toward the discovery of the strength and behavior of fabricated tubular columns such as those commonly used in off-shore oil structures. A series of ten long, fabricated, tubular steel columns, of relatively large diameter, was tested in compression, with essentially pin-ended conditions.

As a preliminary to the testing of the long columns, a number of stub column tests were also made along with an experimental determination of the residual stresses inherent in a typical fabricated tubular column. These residual stresses are both circumferential, due to the process of rolling a tube from a flat plate, and longitudinal, due to welding of the longitudinal pipe seam. Measurement of these stresses is considered essential to any theoretical analysis of column behavior.

The use of spherical bearing heads in long column tests allowed observation of the preferred buckling direction, as well as giving the maximum possible slenderness ratio (kL/r). Detailed observations are made of various factors affecting column buckling behavior, including differing yield stresses within a column specimen, the presence

of longitudinal and horizontal welded seams, initial out-of-straightness, and end rotations.

On the basis of these tests it is found that the current CRC column strength curve may give an unconservative estimate of column strength, if used directly with mill report yield strength values, within the range of slenderness ratios tested ($L/r = 39$ to 83).

TESTS OF FABRICATED TUBULAR COLUMNS

D. A. Ross¹ and W. F. Chen², M. ASCE

1. Introduction

A relatively new development in structural engineering is the use of fabricated, tubular steel beams and columns. This trend is growing particularly in the design of off-shore oil structures, multi-story structures, and off-shore thermal energy conversion structures.

Designers of such structures face an immediate problem in the lack of a reliable design guide, since such columns are usually fabricated in diameters far greater than those for which previous research data is available. This lack of knowledge on the strength of these members, suitably based on experimental evidence, hampers the designer in his efforts to design a safe, but relatively economic, structural member. There is also a more fundamental problem with such structural members, arising due to the lack of knowledge of the behavior of members fabricated by relatively new fabrication processes. Among problems associated with prediction of member behavior are the effects of two-dimensional residual stresses in members introduced during fabrication and the unknown importance of initial imperfections in fabrication.

A research program currently underway at Lehigh University is attempting to provide information which will assist in solving the problems of strength and behavior of such members. The program has both theoretical and experimental phases, both of which attempt to provide design assistance.

¹Research Assistant, Fritz Engineering Laboratory, Lehigh University, Bethlehem, Pa. 18015

²Professor of Civil Engineering, Fritz Engineering Laboratory, Lehigh University, Bethlehem, Pa. 18015

This paper reports the experimental phase of the investigation. Included in the investigation was an experimental determination of residual stresses in a typical fabricated tubular column, the testing of three stub columns, and the testing of ten full-scale long columns under axial load and pin-ended conditions with slenderness ratios ranging from 39 to 83.

2. Scope of Test Program

It is appropriate here to consider briefly the manufacturing process by which fabricated tubular structural members are commonly made in the U.S. Usually the tubular member is formed by cold-rolling flat plate until opposite edges come together. A cylinder, or "can" is then formed by welding down this longitudinal joint. Manufacturing limitations usually limit the length of these cans to about 3 meters (10 ft), but any number of these cans may be welded together, end-to-end, to form the desired member. A possibility of longitudinal weld tearing in a completed member when loaded is avoided by staggering the welds between "cans", usually making the weld in one can about 180° out-of-phase to the weld in the next can. (American Petroleum Institute Specifications (1) require at least 90° out-of-phase.)

The rolling process in manufacture clearly introduces circumferential residual stresses which vary through the thickness of the plate, while the longitudinal welding process introduces longitudinal residual stresses. Particular attention of this research has focussed on the magnitudes and distributions of these stresses, which are a necessary prelude to any analytical investigation of the effects of these stresses on beam-column behavior under load. The measurement was undertaken on a short column, of similar size to that used in the three stub column tests.

The stub column tests were undertaken in order to allow derivation of column buckling strength curves to allow prediction of buckling loads for long columns. The long columns vary in length from 5.5 to 11 meters (18 to 36 ft.) and in diameter from 380 mm (15 in.) to 560 mm (22 in.). An important feature of these tests was the use of spherical end blocks during column testing. Apart from simulating, as closely as possible, pin-ended conditions and thus the longest possible "column effective length", this also allowed a column being tested to determine its own (previously unpredictable) buckling direction.

Table 1 gives the detailed list and dimensions of specimens supplied for testing. The specimens were fabricated in accordance with the requirements of American Petroleum Institute Specifications (1), with welding procedures conforming to American Welding Society (2) requirements. The sections used to form the columns were from A36 steel plate in which the original milling direction was perpendicular to the longitudinal axis of the finished columns. Two heat lots of steel were included in the specimens and the properties of these, as found in various tensile coupon tests and stub column tests, is recorded in Table 2. The wall thickness of all specimens was 7.8 mm (5/16 in.).

3. Preliminary Tests

In this paper it is not intended to detail the common supplementary tests for column testing. The critical material properties, as determined from tensile coupon testing, have already been detailed in Table 2. The stub column tests were conducted in the 5,000,000 lb. Baldwin Testing Machine in the Fritz Engineering Laboratory of Lehigh University, using the technique

reported and recommended in Ref. 11. The column buckling strength curves obtained from these tests will be presented at a later stage in this paper. Detailed derivation of preliminary data is presented in Ref. 8.

Furthermore, it is not proposed to discuss in detail the testing techniques by which the residual stresses were determined, as these are adequately covered in Ref. 9. It is sufficient here to note that a destructive "Whittemore Gage Technique", involving the slicing of a column cross section and measuring changes in strain, was used to measure longitudinal residual stresses. A "hole drilling technique", described in Ref. 7, was used to measure circumferential or "through-the-thickness" residual stresses. Herein, a brief discussion of the results obtained by these testing techniques is presented.

4. Residual Stresses

Longitudinal residual stresses introduced by longitudinal welding of the "cans" were measured by a destructive slicing technique known as the method of dissection into individual bars. The residual stress distribution thus obtained is shown in Fig. 1. Also shown in Fig. 1 are the analytical approximations possible for approximation of the measured stresses. The solid line indicates a possible continuous curve, of the type predicted by Marshall (5). We note that in the region of the weld the material has effectively yielded in tension. As we move further from the weld there are alternating regions of compressive and tensile longitudinal residual stress, of progressively decreasing maximum amplitude. These findings are substantiated by other test results (6).

The dotted straight lines in Fig. 1 represent a proposed straight line approximation to the actual distribution. If x is the distance from the weld, R the tubular member radius, σ_L the longitudinal residual stress at a point, and σ_y the material yield stress, then the following values may be adopted as end points in a straight line approximation:

$$\begin{aligned} \frac{\sigma_L}{\sigma_y} &= 1.0 & \text{at } \frac{x}{R} &= 0 \\ \frac{\sigma_L}{\sigma_y} &= -0.3 & \text{at } \frac{x}{R} &\approx 0.3 \\ \frac{\sigma_L}{\sigma_y} &= 0 & \text{at } \frac{x}{R} &= 1.0 \\ \frac{\sigma_L}{\sigma_y} &= 0.1 & \text{at } \frac{x}{R} &\approx 1.2 \\ \frac{\sigma_L}{\sigma_y} &= 0 & \text{at } \frac{x}{R} &\geq 2.0 \end{aligned} \tag{1}$$

In these equations tensile stress is assumed to be positive. It is necessary of course to insist that the summation of residual axial stresses around the tubular column is zero. In the above approximation, however, no attempt has been made to balance bending moment about an axis perpendicular to the weld, as the out-of-balance moment was found to be negligible. Furthermore, initial imperfection measurements suggest that a "can" may bend within its length, possibly to accommodate any such out-of-balance residual moment.

Some indication of the range of applicability of the straight line approximation of Fig. 1 is necessary before it should be adopted. Reference 6 suggests that the approximation may be adequate for column radii up to a

maximum of about 380 mm (15 in.), that is, for radii in excess of this value, R should be taken as 380 mm (15 in.). This is reasonable when it is considered that a finite amount of heat is added to a "can" in the longitudinal welding process. Reference 6 also suggests there may be a minor dependence of the σ_L/σ_y ratio on the yield strength of the material and the welding procedure used.

Circumferential residual stresses were measured by a hole-drilling technique (7) in which surface measurements were taken of the strain release due to drilling at the base of a small diameter hole in the tubular column wall. Figure 2 gives the results obtained from these tests. No significant variation in circumferential residual stresses was found at different locations on the cross section. Figure 2(b) indicates typical experimental results. The testing technique was shown to have a limited range of validity such that the results near the surface, as well as those taken near the center line of the tube were thought to contain possible inaccuracies. Thus the straight line approximation is dotted in these areas. The hole-drilling experiment was conducted both from inside and outside surfaces of the tubular column. Figure 2(c) shows the average circumferential residual stress pattern obtained.

It is appropriate now to consider the analytical prediction of the circumferential residual stresses. Prior to experimental derivation of the distribution shown in Fig. 2(c), predictions of circumferential stresses had been made (10) as shown in Fig. 3. It is likely that fully plastic yielding of the plate occurs during welding, giving the stress distribution shown in Fig. 3(a). In the manufacturing process the rolled plate is then released,

i.e., allowed to "spring back". It was assumed, therefore, that the section elastically unloaded, a process introducing a stress distribution as shown in Fig. 3(b). The distribution of Fig. 3(b) was derived by assuming that all of the bending moment applied to create the distribution of Fig. 3(a) was released. Addition of Figs. 3(a) and 3(b) gave the predicted circumferential residual stress distribution shown in Fig. 3(c). Figure 4 shows that this prediction differs markedly from the measured distribution [taken from Fig. 2(c)]. It is noted that the possibility of incomplete spring back and subsequent cooling of the welds may partially explain the discrepancies. Furthermore, it is known that the observed results are most suspected in the center line region of the cross section, and the measured results likewise are unlikely to be a good representation.

5. Long Column Testing

5.1 General

In the full-scale long column tests, the maximum nominal length, L , of the column was limited by the height of the Baldwin 5,000,000 lb testing machine in Fritz Engineering Laboratory (about 12 m or 40 ft.), and the minimum column radius, R , (and thus the radius of gyration, r) was controlled by the rolling machine capabilities of the manufacturers.

In the analytical determination of column strength under axial load, a critical parameter is the effective length to radius of gyration (kL/r) ratio. A feature of the present tests was the use of spherical bearing heads at each end of the specimen during testing, in an attempt to provide pin-ended conditions. Not only did this ensure the maximum possible value of k , but it also allowed valuable information on column behavior to

be collected. Unlike a column of I or H section, in which the buckling direction is well defined, it was impossible to predict accurately the buckling direction of a fabricated tubular column. Thus the use of spherical bearing heads allowed each column to adopt its preferred buckling direction, which was then measured.

In any testing it is impossible to attain a true pin-ended condition because of unavoidable frictional resistance to head rotation, and thus a method of measuring the effective column length was necessary. Electric resistance strain gages were mounted on each specimen at quarter points along the specimen length and near each end. A good approximation to the true column effective length of each specimen was found by plotting the curvatures measured along the column length in two perpendicular directions.

It has also been mentioned that two different heat lots of steel were introduced into the specimens, and so the last column of Table 1 specifies which heat lot the material near center of each specimen was made from. This is done since buckling of a specimen is expected near the center of a pin-ended column subjected to axial load.

5.2 Initial Imperfections

At least two types of initial geometric imperfection were considered to have significant influences on column buckling strength and behavior: out-of-roundness and out-of-straightness. Out-of-roundness measurements were made on one fabricated specimen and it was found that, in general, there was less than one percent difference between two perpendicular diameters at a particular position along the column length, which was considered negligible.

These measurements were, therefore, not made on subsequent specimens. It was concluded that out-of-roundness was not a significant parameter in the column performance, due to a high degree of accuracy in manufacture.

The American Petroleum Institute has specifications (1) on the maximum allowable out-of-straightness of a specimen. The specifications allow 3 mm (1/8 in.) in 3 m (10 ft.) (or one part in one thousand), with the restriction that the out-of-straightness not exceed 9 mm (3/8 in.) in 12 m (40 ft.), (or 7.5 parts in ten thousand). Since specimen out-of-straightness can be a critical parameter in determining column performance, particularly in fixing the buckling direction, considerable effort was expended to measure these imperfections.

Clearly there is a problem in establishing diametrical planes on which to take these out-of-straightness measurements. An attempt was made to find an axis of maximum out-of-straightness by rolling the specimen on a flat surface until a position of unstable equilibrium was reached. The longitudinal welds, however, hampered this process, and in general, one of the diametrical planes was established close to these weld locations. The actual out-of-straightness of each specimen was measured with the specimen in an upright position using a theodolite.

A typical resulting out-of-straightness pattern is shown in Fig. 5, for an 11 m long and 0.38 m diameter specimen. The distribution of heat lots along the specimen is shown in Fig. 5, which also shows a diagram exploded along line A to show the relative weld positions. Each weld is fixed at between 25 and 50 mm (1 and 2 in.) from either line A or line C as indicated. Table 3 quantifies the magnitude of the out-of-straightness and also the

form of the out-of-straightness pattern. In general, the API specified tolerances for out-of-straightness have not been exceeded. It appears that the out-of-straightness on a diametrical plane nearly parallel to the weld locations is greater than that on perpendicular diametrical planes.

5.3 Experimental Technique

Lateral deflections at quarter points along the length of each specimen and rotations of the spherical end bearing blocks were measured. Since longitudinal lines had been established on each specimen for out-of-straightness measurements, these lines were also used to establish points on the circumference for measurement of axial strain and lateral displacement.

Rotations in two perpendicular directions of the bottom bearing block could readily be measured manually with a dial gage and spirit level apparatus. (The slope of the base plate could then be measured relative to an arm kept horizontal with the aid of the level.) However, this same procedure was difficult for the head rotation measurements because measurement had to be made at an elevation of up to 12 m (40 ft.). The problem was solved with the use of two plumbob-type rotation gages (to measure two perpendicular rotations) in which the curvature of a sheet metal plumbob support was measured with electric-resistance strain gages (a separate calibration of the gages was required).

Because of the unpredictable direction of lateral movement of the specimen during loading and at buckling, direct measurement of lateral deflection became difficult. The situation is further complicated by the desire to measure deflection of a point on a curved surface. This problem

was solved to an adequate degree of accuracy by constructing a frame on the testing machine at quarter points of the specimen length, such that a long horizontal wire could be attached at one end to a measuring apparatus attached to the frame and at the other end to a point on the specimen. The wire length was of the order of 1.6 to 2.0 m, allowing the assumption that movement perpendicular to the wire produced a negligible effect on the gage reading. The gage could thus be taken to be measuring deflections unidirectionally. The deflections were measured at quarter-points by potentiometers (four at each level) and also at mid-height by dial gages (also four).

Alignment of each test specimen was a further problem. Ideally, alignment is a geometrical condition in which the center of each end of the specimen is aligned with the center of the spherical bearing block at that end. This is quite different to a stub column test in which end alignment may be ensured by a process of trial-and-error loads until equal straining is noted at points on a section circumference. For these tests, the best possible alignment was obtained, and then the remaining unintentional end eccentricity noted. Table 4 gives these measured eccentricities and also attempts to give an indication of the magnitude of these end eccentricities. If the eccentric moment at buckling, M_{ecc} , computed as the product of the buckling load and measured resultant eccentricity, is divided by the fully plastic moment M_p of the section, then the resulting ratio tabulated in Table 4, gives an indication of the relative magnitude of the end moments caused by the unintended initial end eccentricities. This end eccentricity is essential in the theoretical analysis in which the column is treated as a biaxially eccentrically loaded member.

Figure 6(a) shows a typical specimen prior to testing, while Fig. 6(b) shows the same specimen after testing. Maximum lateral deflections measured were of the order of 20 cm, but considerable elastic straightening of the specimen was noted as the applied load was decreased after the test.

The axial load was applied in increments and the static readings of column behavior recorded.

5.4 Results and Discussion

Axial load-lateral deflection curves such as those shown in Fig. 7 were obtained for each specimen at each quarter point along the specimen length. Each of these curves was plotted as an average deflection of two sides of the specimen (with dial gages and potentiometers active at midheight). It was characteristic that for most specimens some lateral movement was noted at approximately 70 to 80% of the maximum recorded load. Furthermore, buckling was a sudden phenomenon, involving the almost instantaneous adoption of large lateral deflections, coupled with a rapid decrease in the load carrying capacity of the column specimen.

In Table 5 some data is given of column behavior at failure, from which a number of interesting conclusions may be formed. The location of the critical section (whether by local buckling or by formation of a plastic hinge with little change in cross sectional shape) occurred frequently at some point well removed from the center of the specimen. It was clearly observable during testing that either a longitudinal weld in one can or the preference of the column to buckle in material of lower yield strength were responsible for this phenomenon. It is considered that the critical load obtained will,

in general become progressively greater than that of a uniform column as the critical section occurs further away from the center of the specimen. Thus the inclusion of longitudinal welds and the insertion of material of higher yield stress at or near the column center was advantageous in column strength and behavior. Specimens 6 and 9 fail at exceptionally large distances from the center of the specimen length. It is noted also that they have other unusual behavior. This will be described later.

Another noteworthy aspect of Table 5 is the buckling direction. In all except one case, the diametrical plane containing the buckling direction makes an acute angle 45° or greater to the diametrical plane containing the weld. In at least five specimens the buckling direction is perpendicular to the diametrical plane containing the longitudinal welded seams. In only one specimen, specimen 4, could the buckling direction be said to be parallel to the plane containing the welds. In this specimen, the bending was such that the welds in the buckling cans were in compression.

The range of (kL/r) ratios tested in this series of experiments encompasses the transition from the mode of local buckling type of failure, recognized by the checkerboard pattern of cross section distortion, to the formation of a plastic hinge as the type of failure mechanism characterized by general yielding of an entire can and relatively little cross section distortion. From the obtained data, a (kL/r) ratio of about 50 is an indication of the transition from local buckling to plastic hinge formation at failure.

It is noted that the critical "can" of column specimen 10 was not the central can. Examination of the out-of-straightness patterns suggests these may have been a factor. The critically yielded "can" of specimens 6

and 9 was located at exceptionally large distances from the center of the specimen length, despite the use of steel from the same heat lot throughout both specimens. Table 5 also shows that both failed in a local buckling mode in somewhat unusual buckling directions. In both cases, the critically yielded zone was only a few inches from a circumferential weld. Examination of the out-of-straightness patterns shows a possibility that this may have been an influencing factor, with greater than average "misfit" between the longitudinal axes of consecutive cans at the critical circumferential welds. Such factors may determine the position of critical "can" along the column length.

Two other aspects of post-buckling column behavior are shown in Table 6. The maximum lateral deflections measured at center of the specimen height are recorded numerically and also as a percentage of the nominal specimen length. It can be seen that maximum lateral deflections of the order of 1.0 to 1.7% of the column length were obtained, and at these deflections the residual axial load carrying capacity of the member was usually of the order of 40% of the critical buckling load.

In Table 6 an attempt is also made to verify the importance of the buckling or post-buckling behavior. In the direction of buckling, the rotation of the top head, θ_T , is recorded as a fraction of the rotation of the bottom head, θ_B . Prediction of this ratio could readily be made by assuming that the buckled column had all plastic rotation concentrated at the critical location, i.e., that the deflected shape of a buckled column was essentially bilinear. Comparison of these observed and predicted values shows good agreement, except for two specimens, for which a relatively important secondary critical location could be found.

Observation of Tables 1 and 5 shows that the larger diameter column specimens all failed in a local buckling mode, and were the only specimens to do so. For the longest of these columns, the failure was initially in formation of a plastic hinge, followed immediately by local buckling. This would suggest that large diameter columns may have difficulty in sustaining finite rotations of a plastic hinge. Local cross sectional distortion is needed to allow such rotations. However, the column buckling strength is not a function of column diameter. There was a sudden, catastrophic loss of axial load-carrying capacity in specimens which failed by local buckling. In contrast, the loss of load-carrying capacity was less sudden when a plastic hinge was formed and a significant plastic hinge rotation capacity was usually observed.

5.5 Comparison of Predicted and Observed Buckling Loads

Figure 8 defines both critical axial load, P_{cr} , and buckling load, P_b , as obtained during experimentation. The buckling load is essentially the maximum static load recorded, whereas the critical load is taken as the maximum load the specimens sustained. Usually the buckling load and critical loads were within 100 kN (22 kip) of each other.

When yield stress values of the steel are considered, a similar rate-dependent phenomenon is evident. It is well known that the higher the strain rate at which the specimens are tested, the higher the obtained yield stress. Herein, we take the mill-report yield stresses as pseudo-dynamic yield stresses, while yield stresses taken after a specified waiting period (as in ASTM A370 specifications) as values of static yield stress. In this paper, results are presented both as buckling load with 'static' yield strength material assumed and critical load with mill-report yield strength material assumed.

In Fig. 9, the three stub column strength curves are presented together with the ten long column test results. Static yield stress values are used in derivation of these curves. These curves give a lower bound on long column strength tests obtained.

Figure 10 presents results compared to two available design column strength curves. The CRC strength curve (4) is commonly used in design computations, and the multiple column curve "a" (3) is a more recent proposal for design of tubular members. Figure 11 plots the same information using static values of yield stress and column buckling load. It can be seen that both proposed design curves may be unconservative in the intermediate range of (kL/r) ratio, i.e., in the range covered by these tests, if mill report yield stresses are used. However, if static yield stresses are used together with column buckling loads, the proposed curves are adequate in this range of (kL/r) ratio. Since there is only minor difference between buckling and critical axial loads, the importance of adopting the correct yield stress is amply illustrated. From Table 2 it can be shown that adoption of mill report yield stresses instead of true static yield stress values provides an increase in yield stress of 17 and 8% for heat lots I and II, respectively, in the test sequence reported herein.

6. Summary and Conclusions

This paper presents a summary of the experimental phase of a research program currently underway in Fritz Engineering Laboratory, Lehigh University. The program is directed toward discovery of the strength and behavior of large fabricated tubular steel columns such as are commonly used in offshore structures. Described herein are various preliminary tests,

including the experimental determination of residual stresses and column buckling predictions based on stub column tests. The major portion of the paper, however, concerns the testing of ten full-scale tubular columns subjected to quasi-static axial loads. A feature of the experiments was the use of essentially pin-ended column conditions, and considerable emphasis is placed on various aspects of column behavior.

The circumferential residual stresses in a tubular column caused by the rolling process used in column manufacture, were found to be as shown in Fig. 2. Figure 3 shows the inaccuracies inherent in a common theoretical assumption of the form of this stress distribution, which may have been inaccurate because of incomplete "springback" in tube manufacture. A longitudinal welding process by which a rolled plate is made into a cylindrical tube is found to introduce longitudinal residual stresses with a distribution of the form shown in Fig. 1. Linear approximation of this was attempted since values of these residual stresses are essential to any theoretical analysis of long column behavior.

A series of ten long, relatively large, fabricated, tubular columns was tested in the 5,000,000 lb Baldwin Testing machine in Fritz Engineering Laboratory. The use of spherical end blocks not only provided essentially pin-ended conditions and thus the maximum possible (kL/r) ratio, but also allowed observance of the buckling direction--an unknown previously. For each specimen, initial out-of-straightness was measured prior to testing, and sufficient data was accumulated to allow subsequent derivation of axial load-lateral deflection curves, column effective lengths, and end rotations of the specimen.

The range of (kL/r) ratios tested encompasses the transition of failure mode from local buckling, characterized by checkerboard cross sectional distortion of the critically yielded location, to plastic hinge formation, characterized by general yielding of a more extensive area and less cross sectional distortion at buckling. The buckling direction in the critical "can" frequently tended to be in a plane approximately perpendicular to a diametrical plane containing the weld, but this was not universally true. Out-of-straightness could be shown to be a significant parameter only infrequently, due possibly to the frequent occurrence of double and triple curvature. There appear to be certain beneficial aspects of the manufacturing method currently adopted. Since an perfect column may be expected to buckle near the center of its length, the degree to which this location has been displaced from the center is some measure of the increase in strength generated. The critical "can" location is usually displaced by the presence of "can" of lower yield strength at a distance from the midheight of the column, and also by a desire to place the longitudinal welded seam in an area of low bending stress.

Comparison of existing column strength curves with experimental results is presented in Figs. 9, 10 and 11. In the intermediate range of (kL/r) ratio tested the stub column tests were shown to adequately predict the lower bound of column strength. However, the two proposed column strength curves for use in design of long columns only give conservative results if a true static yield stress value is assumed for the material, in contrast to the pseudo-dynamic nature of classical mill report tests.

7. Acknowledgments

The investigation reported herein is being conducted in Fritz Engineering Laboratory, Lehigh University, Bethlehem, Pa. Dr. L. S. Beedle is Director of the Laboratory.

The experimental phase of the research was supported by the American Petroleum Institute through the Column Research Council. The theoretical phase of the work is currently supported by a grant from the National Science Foundation to Lehigh University.

The interest, encouragement and guidance of the Advisory Committee, of which Mr. L. A. Boston is Chairman, is gratefully acknowledged.

8. References

1. API Specification for Fabricated Structural Steel Pipe, American Petroleum Institute, API Specification 2B, October 1972.
2. AWS Specification for Welded Highway and Railway Bridges (AWS D1.1-72) American Welding Society.
3. Bjorhovde, R., "Deterministic and Probabilistic Approaches to the Strength of Steel Columns," dissertation presented to Lehigh University, Bethlehem, Pa., in partial fulfillment of the requirements for the degree of Doctor of Philosophy, May 1972.
4. Johnston, B. G., editor, "The Column Research Council Guide to Design Criteria for Metal Compression Members," second edition, Wiley, 1966.
5. Marshall, P. W., "Stability Problems in Offshore Structures," presentation at the Annual Technical Meeting of the Column Research Council, St. Louis, March 25, 1970.
6. Ostapenko, A. and Gunzelman, S. X., "Local Buckling Tests on Two High Strength Steel Tubular Columns," Fritz Engineering Laboratory Report No. 406.2, Lehigh University, Bethlehem, Pa., July 1975.
7. Redner, S., "Measurement of Residual Stresses by the Blind Hole Drilling Method," Photolastic, Inc., Bulletin TDG-5, 1974.

8. Ross, D. A. and Chen, W. F., "Stub Column Tests, Tensile Coupon Tests and Preliminary Predictions of Column Buckling Strength," Fritz Engineering Laboratory Report No. 393.5, Lehigh University, Bethlehem, Pa., January 1976.
9. Ross, D. A. and Chen, W. F., "The Axial Strength and Behavior of Cylindrical Columns," paper No. OTC 2683 presented to the Eighth Annual Offshore Technology Conference, Houston, Texas, May 3-6 1976.
10. Ross, D. A. and Chen, W. F., "Theoretical Analysis of a Short Biaxially Loaded Tubular Column," Fritz Engineering Laboratory Report No. 393.2, Lehigh University, Bethlehem, Pa., April 1975.
11. Tall, L., "Stub Column Testing Procedure," Document C-282-61, Class C Document, International Institute of Welding, Oslo, June 1962; also, appendix to "Column Research Council Guide", second edition, edited by B. J. Johnston, Wiley, 1966.

9. List of Symbols

D_o	= nominal outside diameter of column
E	= modulus of elasticity
k	= effective length factor
L	= column length
M_{ecc}	= maximum eccentric bending moment
M_p	= fully plastic bending moment of cross section
P_b	= buckling load, see Fig. 8
P_{cr}	= critical axial load, see Fig. 8
P_y	= yield axial load
R	= column radius
r	= radius of gyration
x	= distance from base of specimen
t	= wall thickness
δ_E	= end eccentricity in eastern direction

- δ_N = end eccentricity in northern direction
- σ = stress
- σ_y = yield stress
- σ_L = longitudinal residual stress
- σ_c = circumferential stress
- θ_B = bottom head rotation
- θ_T = top head rotation
- $\lambda = \frac{1}{\pi} \sqrt{\frac{\sigma_y}{E}} \frac{L}{r}$

Table 1 List of Specimens

Specimen Number	Nominal Length m(ft)	Effective Length of Buckling m(ft)	Effective Length Factor k	Outside Diameter D cm(in)	Control Heat Lot ^a
1	5.5(18)	5.2(17)	0.95	38(15)	I,II ^b
2	5.5(18)	5.2(17)	0.95	38(15)	I,II ^b
3	7.6(25)	6.7(22)	0.86	38(15)	II
4	7.6(25)	7.3(24)	0.93	38(15)	II
5	7.6(25)	5.2(17)	0.68	56(22)	II ^c
6	7.6(25)	5.8(19)	0.76	56(22)	II ^c
7	11(36)	11.0(36)	1.00	38(15)	II
8	11(36)	7.6(25)	0.69	38(15)	I,II ^b
9	11(36)	8.9(29)	0.81	56(22)	II ^c
10	11(36)	8.5(28)	0.78	56(22)	II ^c

^aThe yield stress of Heat Lot II was higher than for Heat Lot I

^bCircumferential weld near center, different heat lots on each side

^cAll pipe Heat Lot II

Table 2 Material Properties

Origin		I	II
Mill Report	Dynamic σ_y , MPa(ksi)	318(46.1)	328(47.5)
	Static σ_y , MPa(ksi)	---	---
	E, MPa(ksi)	---	---
"Static" Laboratory Test ^a	Dynamic σ_y , MPa(ksi)	288(41.7)	321(46.5)
	Static σ_y , MPa(ksi)	271(39.3)	308(44.6)
	E, MPa(ksi)	211,000(30,600)	212,000(30,700)
ASTM A370 Test	Dynamic σ_y , MPa(ksi)	293(42.5)	324(47.0)
	Static σ_y , MPa(ksi)	271(39.3)	308(44.6)
	E, MPa(ksi)	214,000(31,000)	213,000(30,800)

^a maximum strain rate = 0.64 mm/min (0.025 in/min)

Table 3 Column Specimen Out-of-Straightnesses

Specimen Number	Form of Curvature	Out-of-Straightness (mm/m) ^a	Length of Specimen Considered m(ft) ^a	Form of Curvature	Out-of-Straightness (mm/m) ^a	Length of Specimen Considered m(ft) ^a
1	Single	1.31	4.3(14)	Single	0.5	2.4(8)
2	Local Imperfection Near Weld	2.0	2.1(7)	Local Imperfection Near Central Weld	2.0	2.4(8)
3	Single	1.0	6.1(20)	Single	0.5	6.1(20)
4	Single	0.62	6.1(20)	Single	0.83	4.6(15)
5	Single	0.32	5.5(18)	Single	0.65	5.5(18)
6	Double	0.63	3.7(12)	Triple	0.75	3.0(10)
7	Triple	0.91	7.0(23)	Local Imperfection Near End	1.71	2.1(7)
8	Double	1.18	5.8(19)	Single	0.67	7.6(25)
9	Triple	1.41	4.9(16)	Triple	0.63	5.8(19)
10	Triple	1.45	4.6(15)	Single	1.25	3.0(10)

^aAPI Specification (1) allows 1.0 mm/m every 3 m

Table 4 Unintended Initial End Eccentricities
(Center of Pipe Relative to End Block)

Specimen Number	Top Head			Bottom Head		
	δ_E mm(in)	δ_N mm(in)	$\frac{M_{ecc}}{M_p}$	δ_E mm(in)	δ_N mm(in)	$\frac{M_{ecc}}{M_p}$
1	---	---	---	---	---	---
2	---	---	---	0	-1.0(-0.04)	0.001
3	---	---	---	-2.0(-0.08)	0	0.002
4	-1.5(-0.06)	-1.5(0.06)	0.002	---	---	---
5	0	-7.9(-0.31)	0.045	0	0	0
6	4.8(0.19)	3.3(0.13)	0.029	-1.5(-0.06)	0	0.008
7	10.4(0.41)	4.8(0.19)	0.083	4.8(0.19)	0	0.034
8	-7.9(-0.31)	0.8(0.03)	0.062	0	0	0
9	0.8(0.03)	-1.5(-0.06)	0.009	-4.8(-0.19)	10.4(-0.41)	0.064
10	9.7(0.38)	0	0.053	-2.3(-0.09)	3.3(0.13)	0.022

Table 5 Failure Mechanism and Direction

Specimen Number	Failure Mode	Location of Critical Section $\left(\frac{x}{L}\right)^a$	Direction of Buckling w.r.t. Weld	Remarks
1	plastic hinge	0.48	50-60° to weld	in lower yield strength can
2	plastic hinge	0.48	70° to weld	in lower yield strength can
3	plastic hinge	0.57	perpendicular to weld	in lower yield strength can
4	plastic hinge	0.62	parallel to weld	initial buckle in lower yield strength can
5 ^{then}	plastic hinge, local buckling	0.38	perpendicular to weld	out of central can to avoid high compression in weld
6	local buckling	0.82	60-70° to weld	out of central can to avoid high compression in weld
7	plastic hinge	0.41	perpendicular to weld	in lower yield strength can
8	plastic hinge	0.64	45° to weld ^b	weld in tension in lower yield strength can
9	local buckling	0.27	60-90° to weld ^b	buckle in lower can to avoid weld in compression
10	local buckling	0.56	perpendicular to weld	in upper can no immediate reason obvious

^a x measured from base of specimen

^b out-of-straightness may be a factor in determining buckling direction of these specimens

Table 6 Failure Behavior Data

Specimen Number	Maximum Measured Deflection at Center δ_m mm (in)	$\frac{\delta_m}{L}$ $\times 10^2$	Top End Rotation, θ_T Bottom End Rotation, θ_B	Predicted $\left(\frac{\theta_T}{\theta_B}\right)$
1	53(2.07)	0.96	---	---
2	57(2.24)	1.04	0.70 ^b	1.0
3	84(3.31)	1.10	1.15	1.33
4	96(3.79)	1.26	1.01 ^c	1.63
5	79(3.10)	1.03	0.67	0.61
6	49(1.92) ^a	---	4.42 ^b	4.56
7	184(7.26)	1.68	0.57	0.70
8	140(5.50)	1.27	1.53	1.78
9	106(4.16) ^a	---	0.32	0.37
10	121(4.77)	1.10	1.74 ^c	1.27

^aMaximum deflection closer to a quarter-point

^bApproximation taken up to 20° from the buckling direction

^cExperimental evidence that bilinear approximation inadequate

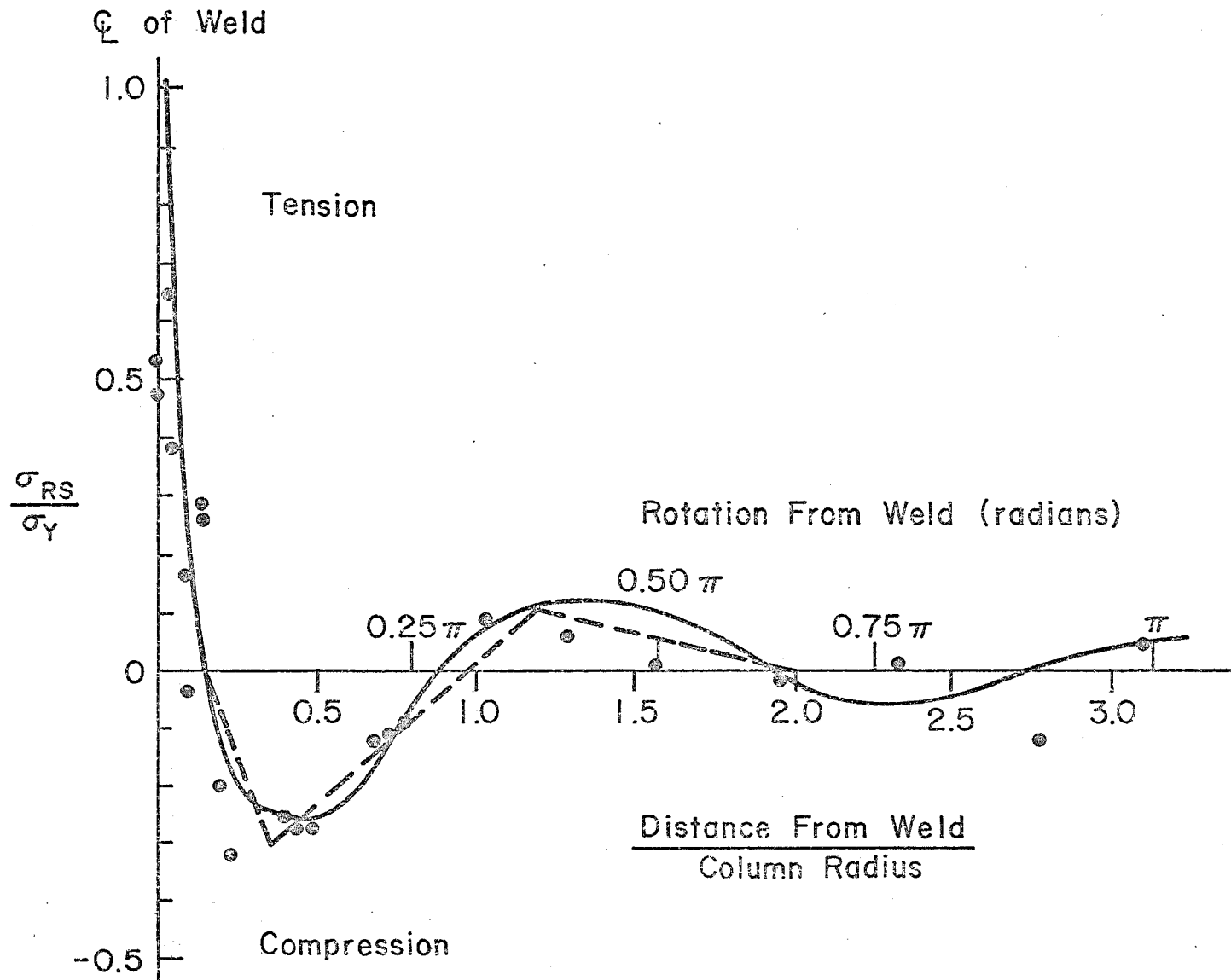


Fig. 1 Longitudinal Residual Stress Distribution Obtained from Slicing Method

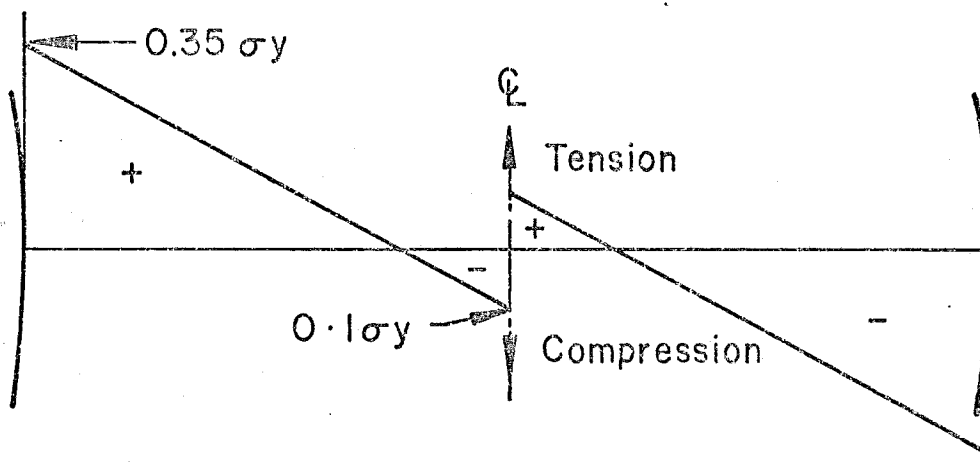
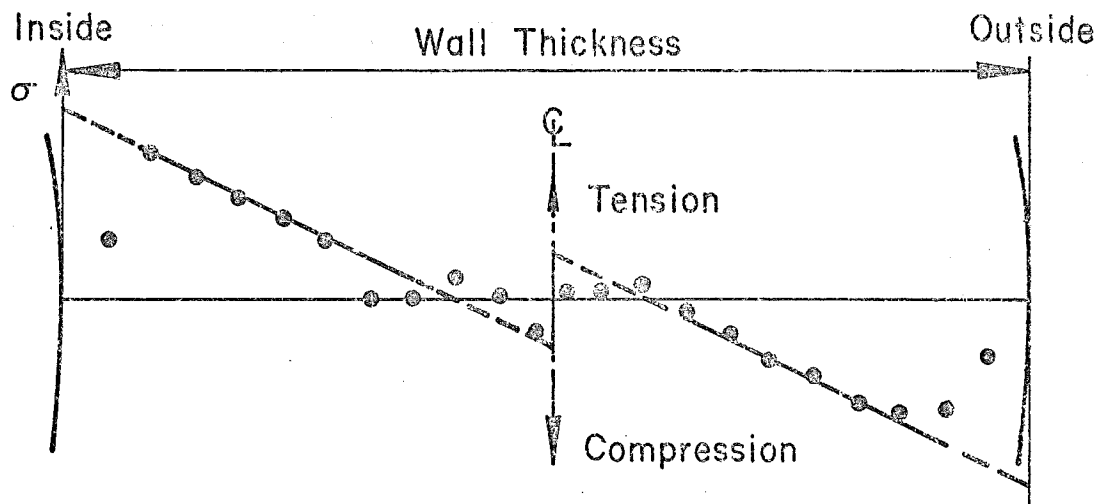
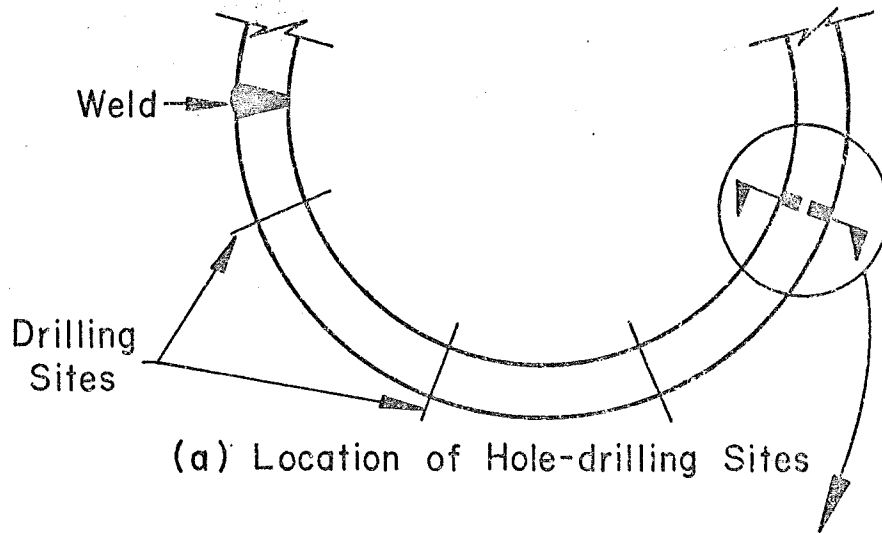
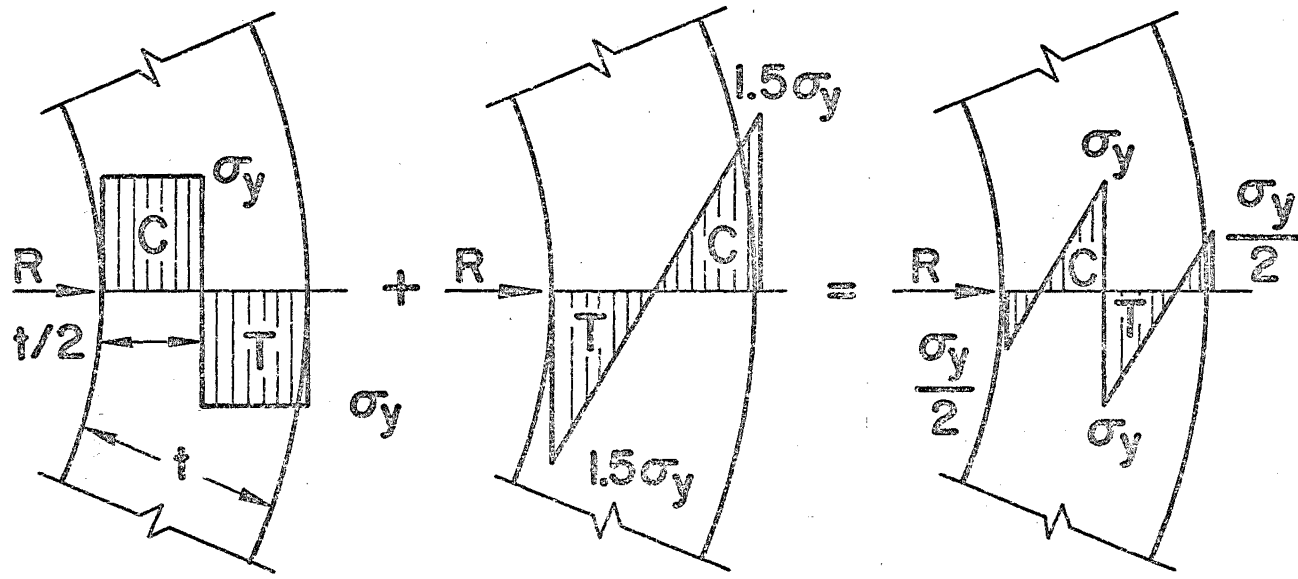


Fig. 2 Circumferential Residual Stress Pattern



**a) FULLY - PLASTIC
PLATE BENDING**

**b) ELASTIC
UNLOADING**

**c) ASSUMED
DISTRIBUTION**

Fig. 3 Circumferential Residual Stress Distribution

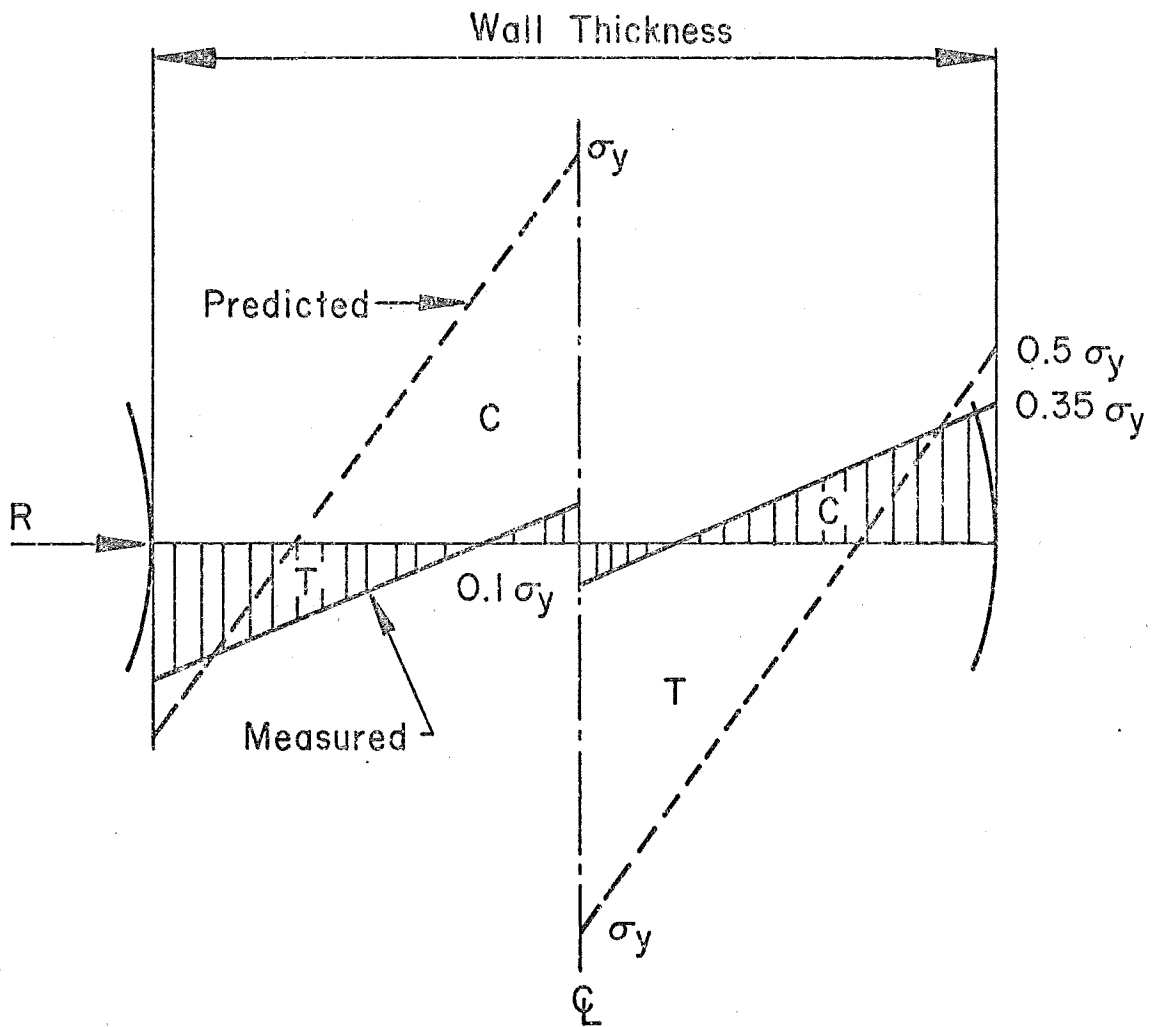


Fig. 4 Comparison of Predicted and Measured Circumferential Residual Stresses

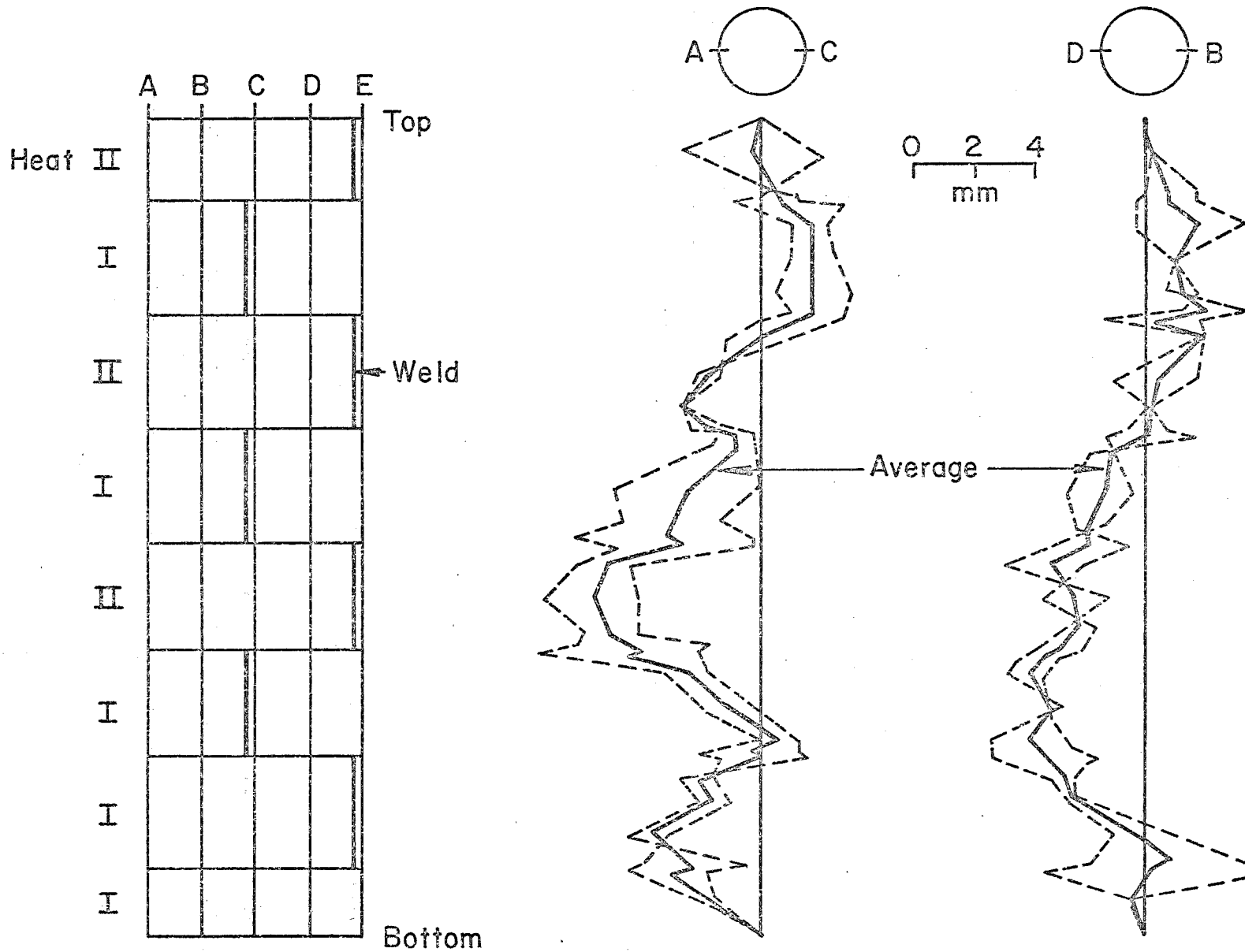
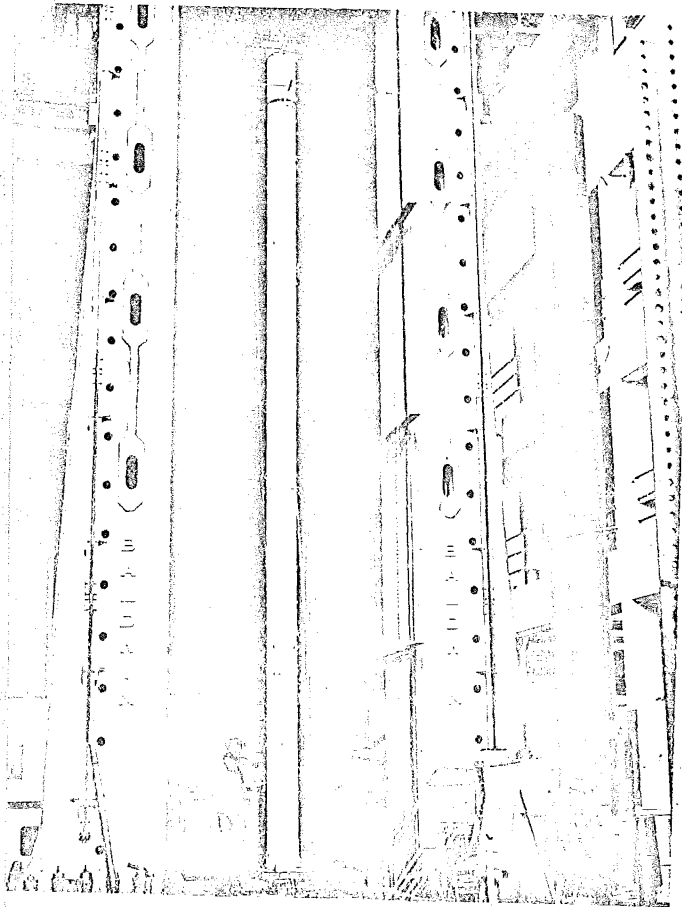
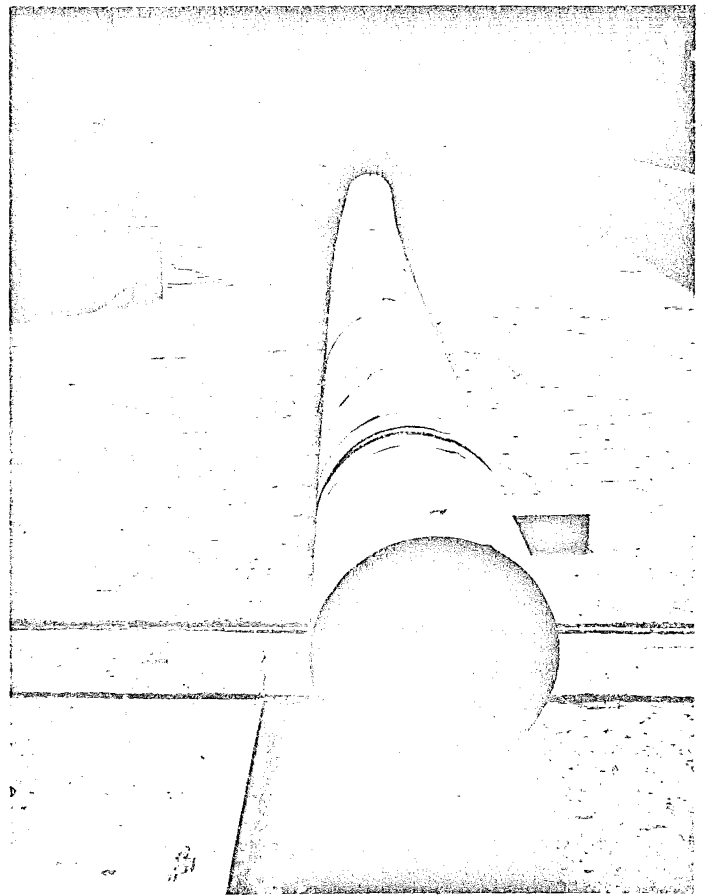


Fig. 5 Typical Specimen Out-of-Straightness as Measured Prior to Testing



a) Column Prior to Testing
(11m x 0.38m Diameter Specimen)



b) Buckled Column After Testing

Fig. 6 Column Testing

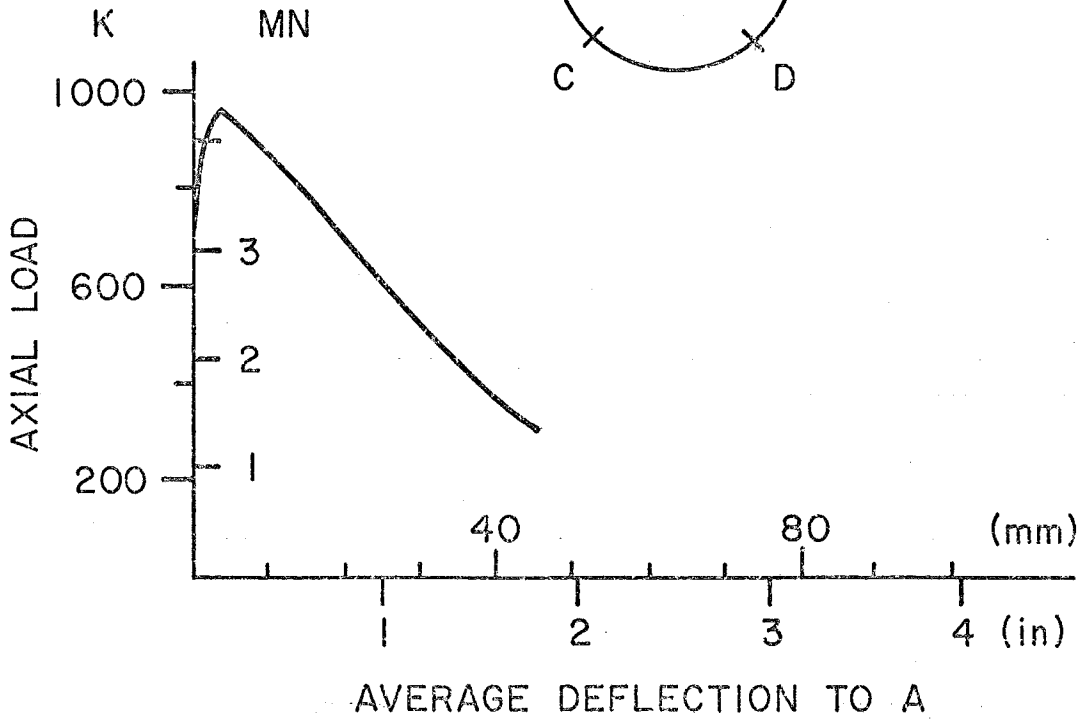
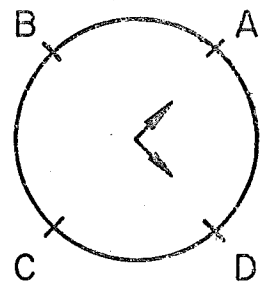
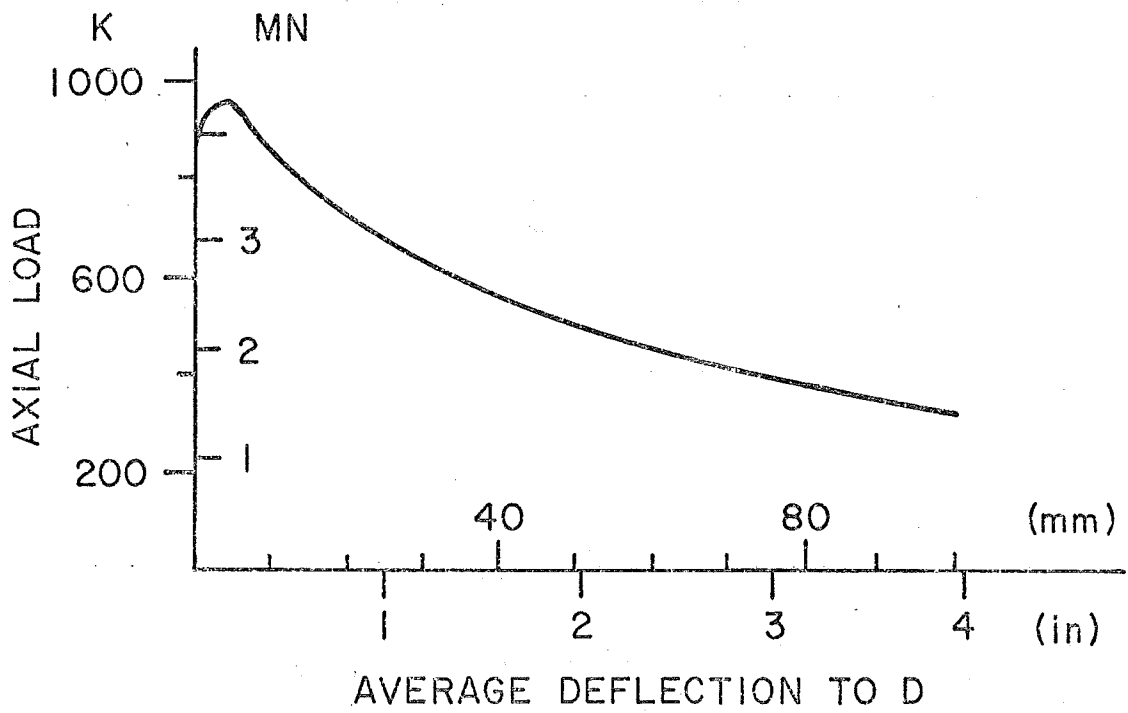


Fig. 7 Axial Load-Lateral Deflection Curves at Midheight

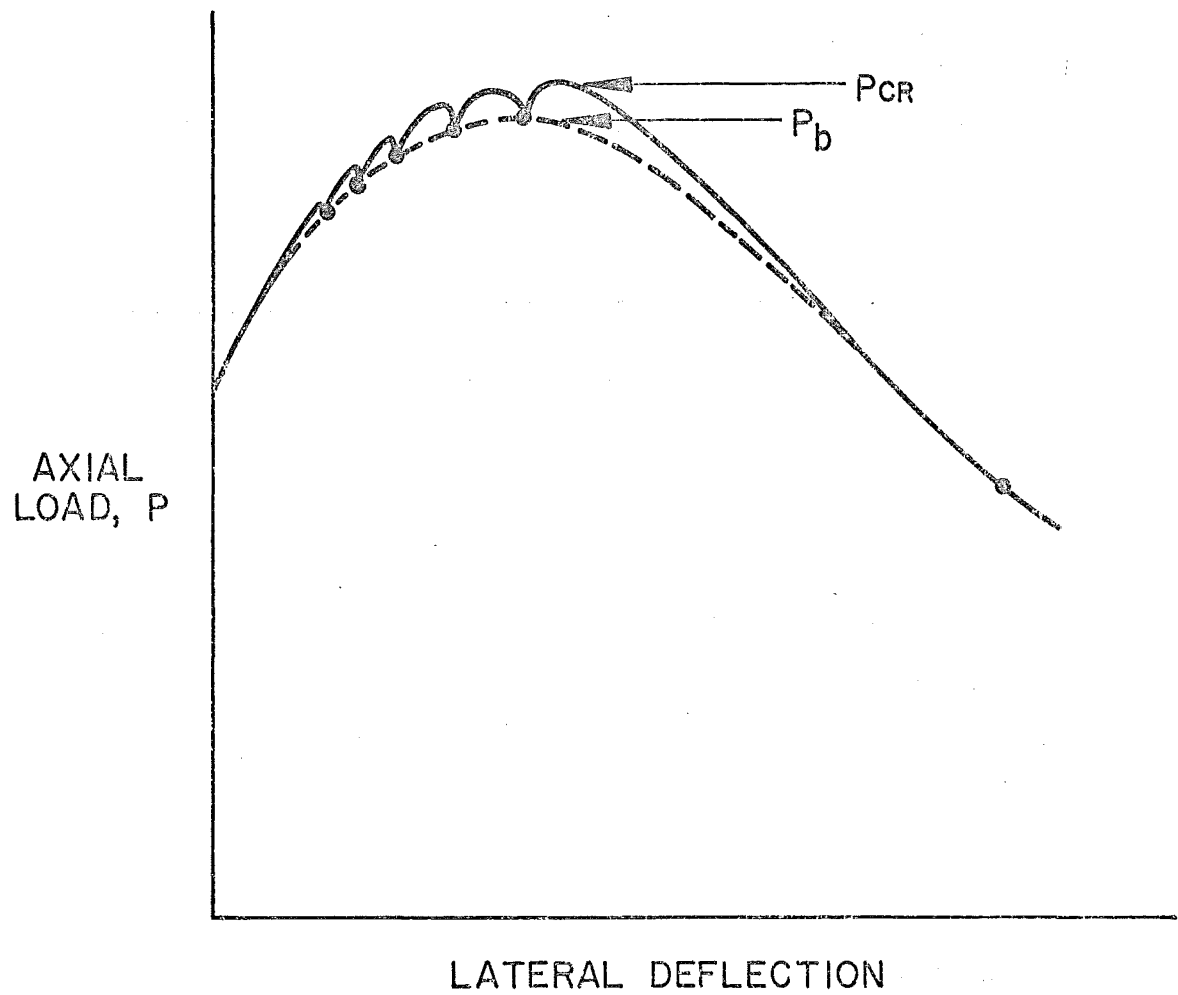


Fig. 8 Definition of Critical and Buckling Loads

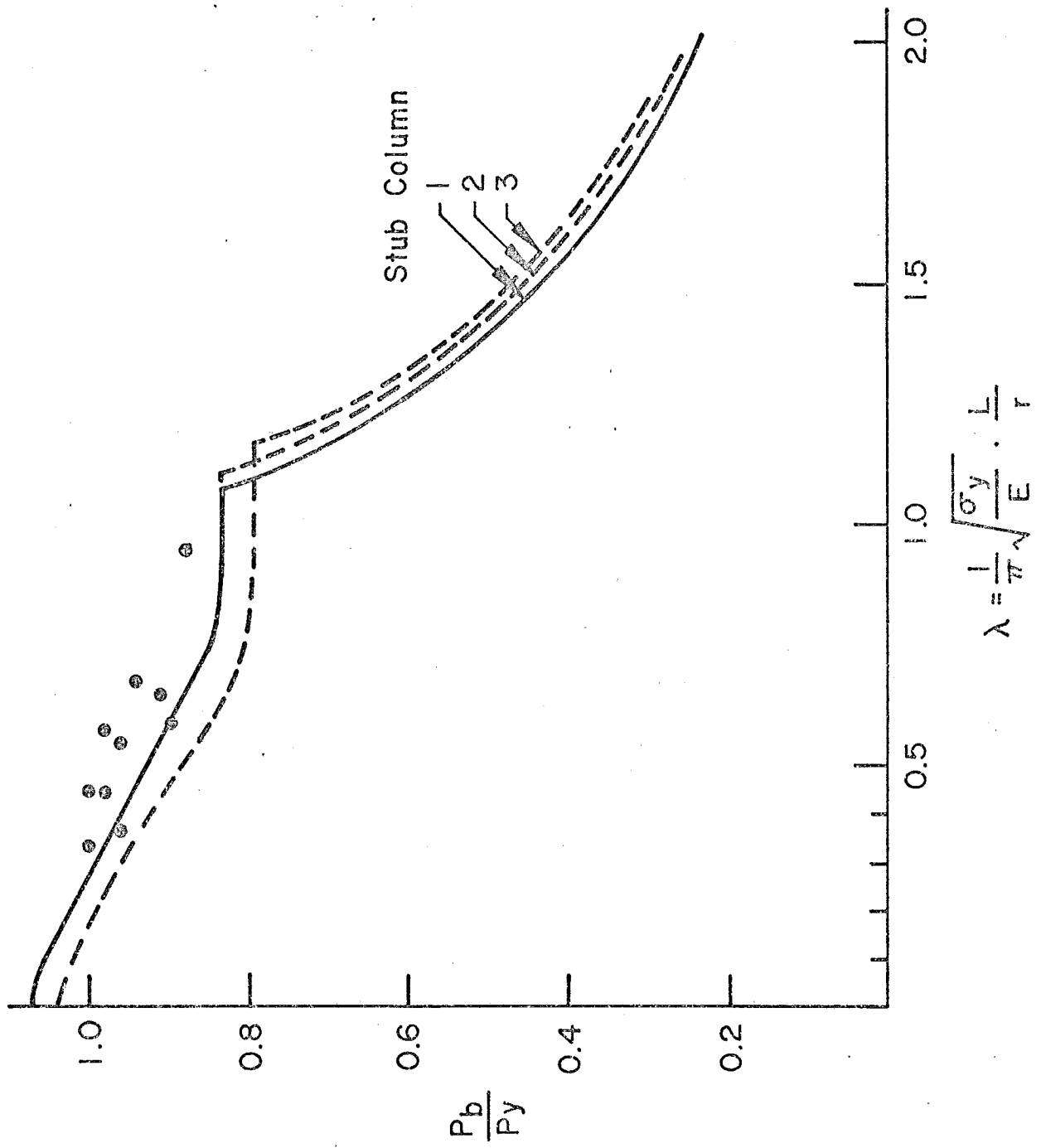


Fig. 9 Stub Column Predictions - Static Yield Stresses Assumed

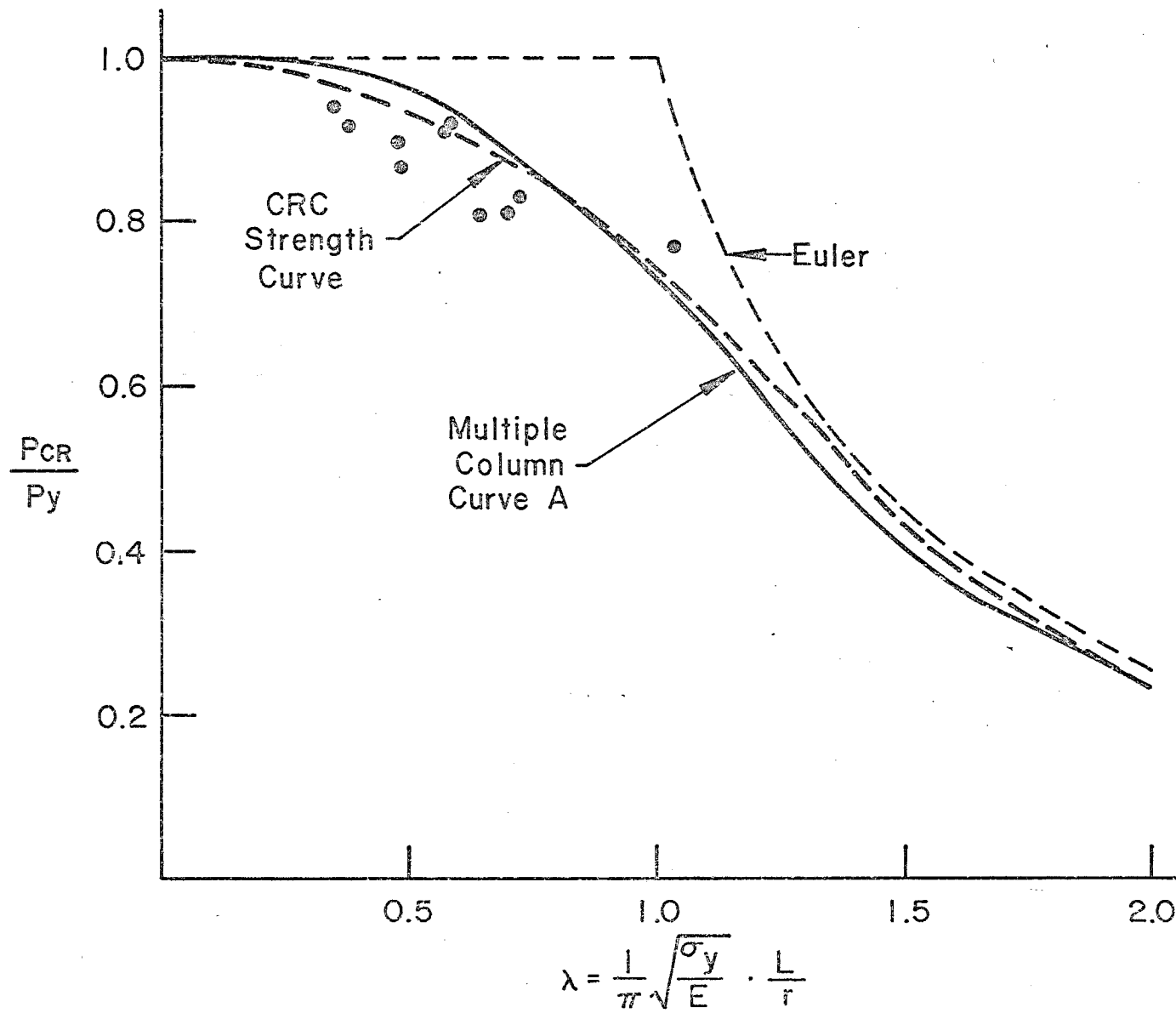


Fig. 10 Comparison of Test Results with Column Buckling Curves - Dynamic Yield Stresses Assumed

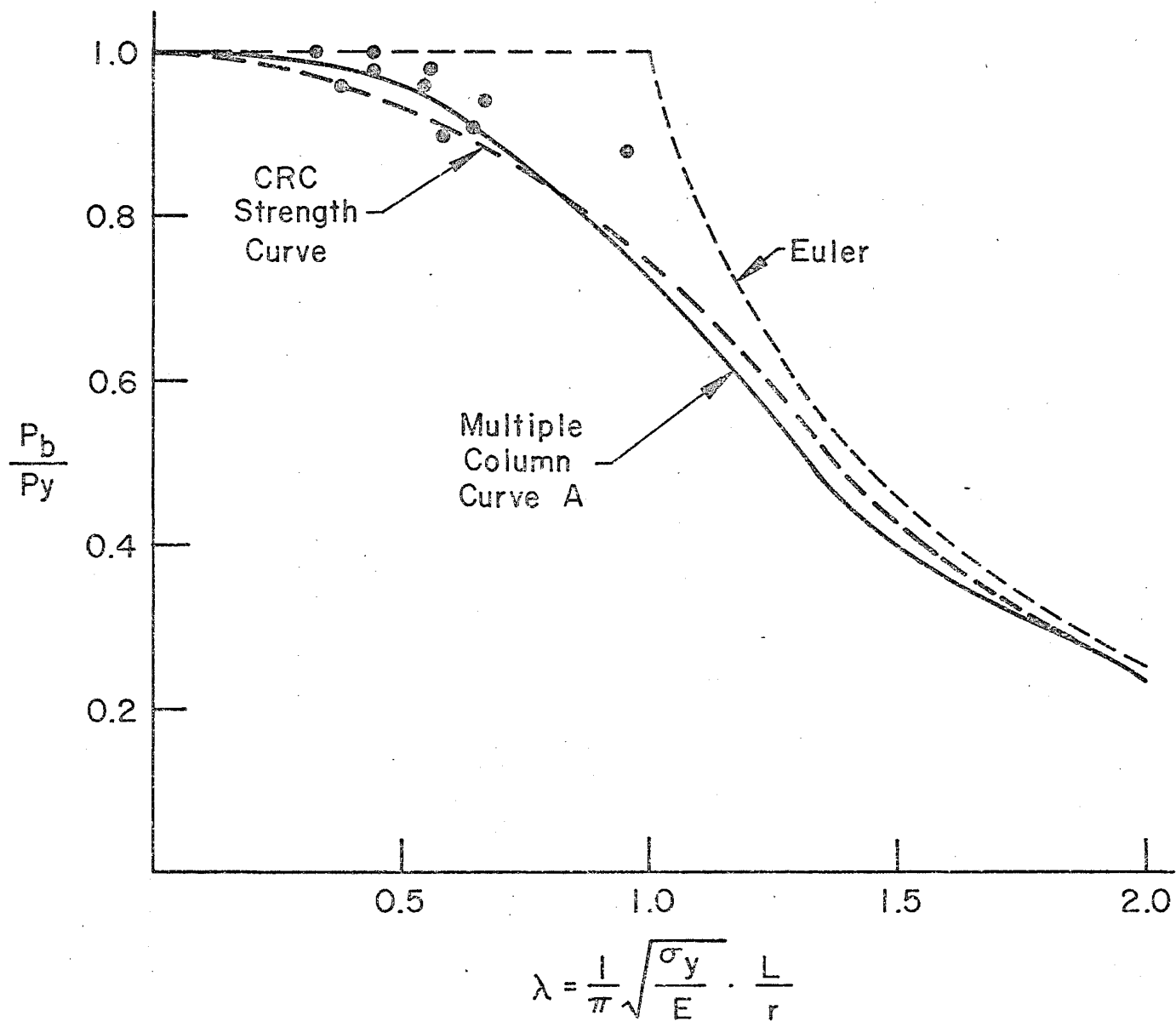


Fig. 11 Comparison of Test Results with Column Buckling Curves - Static Yield Stresses Assumed